Journal of Applied Polymer Science

Reduced percolation concentration in polypropylene/expanded graphite composites: Effect of viscosity and polypyrrole

Jürgen Pionteck,[1] Elixana Maria Melchor Valdez,[1,2] Francesco Piana,[1,3,4] Mária Omastová,[5] Adriaan Stephanus Luyt,[6] Brigitte Voit[1,3]

[1]Leibniz Institut für Polymerforschung Dresden e.V., Hohe Straße 6, 01069 Dresden, Germany
[2]Universidad Simón Bolívar, Valle de Sartenejas, Baruta Estado Miranda, Venezuela
[3]Technische Universität Dresden, Organic Chemistry of Polymers, 01062 Dresden, Germany
[4]Present address: Institute of Macromolecular Chemistry, AV ČR, v. v. i., Heyrovského nám. 2 162 06, Prague 6, Czech Republic
[5]Polymer Institute, SAS, Dúbravska cesta 9, Bratislava 84541, Slovakia
[6]University of the Free State, Qwaqwa campus, Private Bag X13, Phuthaditjhaba 9866, South Africa
Correspondence to: J. Pionteck (E-mail: pionteck@ipfdd.de)

ABSTRACT: With the goal to obtain material combining electrical and thermal conductivity at low filler loadings, composites based on polypropylenes (PP) and expanded graphite (EG) have been prepared. The effects of matrix viscosity and of coating the EG particles with polypyrrole (PPy, EG/PPy = 37.5/62.5 by weight) on the EG dispersibility and formation of percolation structures have been analyzed. When increasing the EG amount from 6 to 8 wt %, the electrical conductivity of PP/EG composites increased by 7–9 orders of magnitude, independent of matrix viscosity. When EG-PPy is added, percolation was observed between 8 and 12 wt % EG-PPy (3 and 4.5 wt % EG) in case of PP with higher viscosity and 6 wt % EG (2.25 wt % EG) in case of PP with lower viscosity, exhibiting a strong synergistic effect of EG and PPy in the latter case. In contrast, PPy does not contribute to reduction of thermal percolation concentration. Thermal percolation is observed at 8 wt % EG in PP/EG composites, but no percolation was found in PP/EG-PPy composites with EG-PPy contents of up to 20 wt %, corresponding to 7.5 wt % EG. Analyzing the melt rheology it becomes clear that the contribution of PPy to the formation of a filler network is strongly dependent on the matrix viscosity. The comparison of thermal, electrical and rheological percolation reveals that PPy participates in electron transport reducing the electrical percolation but not to heat transport. Overall, we found a good correlation between electrical, thermal, and melt rheological percolation concentrations. © 2015 Wiley Periodicals, Inc. J. Appl. Polym. Sci. **2015**, *132*, 41994.

KEYWORDS: composites; graphene and fullerenes; morphology; nanotubes; polyolefins; properties and characterization

Received 18 July 2014; accepted 12 January 2015
DOI: 10.1002/app.41994

INTRODUCTION

By addition of electrical or thermal conductive fillers to intrinsically non-conductive polymers, composites suitable for application e.g. in antistatic housing, as heat exchangers or antistatic and conductive coatings can be obtained. When using nanoparticles their high surface area additionally affects the material properties of the matrix polymer due to a large degree of interactions, which may improve the heat stability, hardness, stiffness, strength, and other material parameters. The most important challenge in the production of electrically conductive composites with acceptable material properties is to obtain the best possible dispersion without losing the contacts among the conductive filler particles, so that conductive paths through non-conducting polymer matrix can be formed. For that a certain filler concentration is necessary, the so-called percolation threshold or percolation concentration (PC). A sudden increase in electrical conductivity σ is observed when increasing the filler amount above this concentration.[1,2] Due to the high difference in electrical conductivity of electrically conductive filler (σ_f) and insulating polymer matrix (σ_p), the overall conductivity of the composite is practically determined just by the filler and its dispersion, and the percolation threshold can easily be detected.

Due to the generally smaller difference in thermal conductivity of the polymer matrix (κ_p) and filler (κ_f), compared to the electrical conductivity differences, no strong percolation effects are detectable in polymer-filler composites. However, different models describe the composite thermal conductivity in dependence of filler degree, assuming two extremes based on the layer model developed by Salazar.[3] In the one extreme the composite can be described as a set of parallel layers oriented

perpendicular to the heat flow, and in the other extreme the parallel layers are oriented in the direction of heat flow. The resulting thermal conductivities $\kappa_{\perp}$ and $\kappa_{||}$, respectively, can be expressed by

$$\kappa_{\perp} = 1/[(1-\varphi)/\kappa_p + \varphi/\kappa_f] \quad (1)$$

$$\kappa_{\|} = \kappa_p(1-\varphi) + \kappa_f\varphi \quad (2)$$

where φ is the volume fraction of the filler. $\kappa_{\perp}$ corresponds to a composite morphology without percolating paths, while $\kappa_{||}$ corresponds to a perfect percolating system. Of course, in real composites thermal conduction occurs as mixed mode of these extremes. Furthermore, in such composites the thermal conductivity is due to phonon transport, while the electrical conductivity is due to electron transport. In non-percolating morphologies, the phonon, a particle-like vibrational state, has to overcome the phase boundaries between the highly conductive particles and the nonconductive polymer matrices, typically connected with scattering losses. Thus, the overall thermal conductivity is also dependent on scattering loss at the interfaces. Since at the same filler concentration smaller sized particles mean more interfaces, it explains the observed fact that bigger filler particles generate higher thermal conductivity than the small particles. Especially, when the particle size is in the range or even smaller than the phonon free path, scattering at interfaces increases the overall thermal resistance.[4] To reduce the boundary resistance due to scattering, strong interactions between filler and matrix are favorable, e.g. due to grafting reactions.[5] In summary, one can expect a fast increase in κ above the percolation threshold, and a moderate one below PC.

The formation of a percolating network also results in changes in the rheological parameter of the composite melts. At PC the elasticity improves due to the formation of a physical network, so that the storage modulus G′ increases drastically with increasing filler concentration above PC. At the percolation concentration, expanded graphite forms three dimensional house-of-card structures in cycloolefin copolymers at a PC of 3.7 wt %. This is much less than that of graphite (17.7 wt %),[6] which could easily be detected by the so called "van Gurp-Palmen plot."[7] However, one should note that the transition from liquid-like to solid-like behavior depends strongly on the temperature of the melt. Pötschke *et al.*[8] found, when analyzing the rheological percolation of multi-wall carbon nanotubes in polycarbonate, a shift of PC from 0.5 wt % to 5 wt % when increasing the temperature for rheological analysis from 170°C to 280°C.

In general, the percolation concentration is dependent on the nature of the filler (size, shape factor,[9] contact surface area,[10] etc.) and the process conditions.[11] To introduce conductivity to our samples we used expanded graphite (EG), a structural modification of graphite.[12] The shape coefficient is very low and a high EG concentration is not required to obtain a good conducting composites.[13] Li *et al.* compared the percolation concentration of EG in PP with those of carbon nanotubes (CNT), carbon fibres (CF) and carbon black (CB) by measuring the electrical and melt rheological properties and found the expected order in percolation concentrations $PC_{(CB)} > PC_{(EG)} > PC_{(CF)} > PC_{(CNT)}$.[14] EG is produced by intercalation[15] or oxidation[16] of graphite and subsequent thermal reduction at a high temperature, usually above 1000°C.[17] This sudden and violent expansion generates a porous worm-like structure [Figure 1(a)], suitable for easy dispersion in a polymer matrix.

The insertion of expanded graphite into PP modifies the matrix microstructure and this can influence not only the physical properties of the material, but also the formation of the percolation path.[18] The crystalline structure changes since EG promotes the nucleation of the ß-form, increasing the crystallization rate and temperature during the cooling process.[19] EG influences the thermal behavior and even reduces the coefficient of thermal expansion.[18] Only 1 vol.% is enough to increase significantly the flexural modulus and impact strength of PP.[20] The viscosity of polymer melts also increases strongly in presence of EG.[21] When properties change significantly in value or tendency above a certain EG concentration, this is due to the formation or stabilisation of an EG network.[22]

In part of this work, we used EG coated with PPy. The coating of EG with PPy changes the surface structure to a more rough morphology, thus increasing the physical and also chemical interactions to the matrix. This may be helpful for the EG dispersion and since PPy is an intrinsic electrically conductive polymer it should contribute to the electrical conductivity of the composite. The conductivity of PPy depends on the doping during the oxidative coupling polymerisation. An excess of oxidative agent introduces positive charges in the polymer chains. The positive charges are compensated by counter ions, typically from the oxidative agent or an ionic surfactant.[23] PPy itself is suitable to modify the electrically properties of isolating polymers.[24] The coating of inorganic or organic particles like carbon nanotubes,[25] silicates or polymeric particles with PPy widens the field of possible applications of PPy.[26] Thus, the possibility to form PPy with various morphologies by using 2D platelet-like templates,[27] 3D spheres[28] or 1D rods[29] makes PPy an important building block in nanotechnology and nanoengineering. The use of PPy coated inorganic carriers as modifiers of the electrical properties of polymer matrices has the advantage that the amount of PPy necessary for the formation of conductive paths can be drastically reduced and that the stability of the percolating paths during processing is increased. The PPy modification of EG gives the possibility that the PPy contributes to the conductive network, as shown for the system PP modified with PPy coated clay.[30,31]

In this work, we analyzed the formation of percolating networks in composites based on PP as polymer matrix containing pure EG or EG modified with intrinsically conductive PPy as filler. For determination of percolation concentration, we characterized different properties of prepared materials. The goal was to see if there is a correlation and what are the differences between electrical, thermal, rheological and mechanical percolation. Furthermore, we studied the influence of different matrix viscosity on the formation of percolating pathways, and if the presence of PPy in the system contributes to the percolating structures.

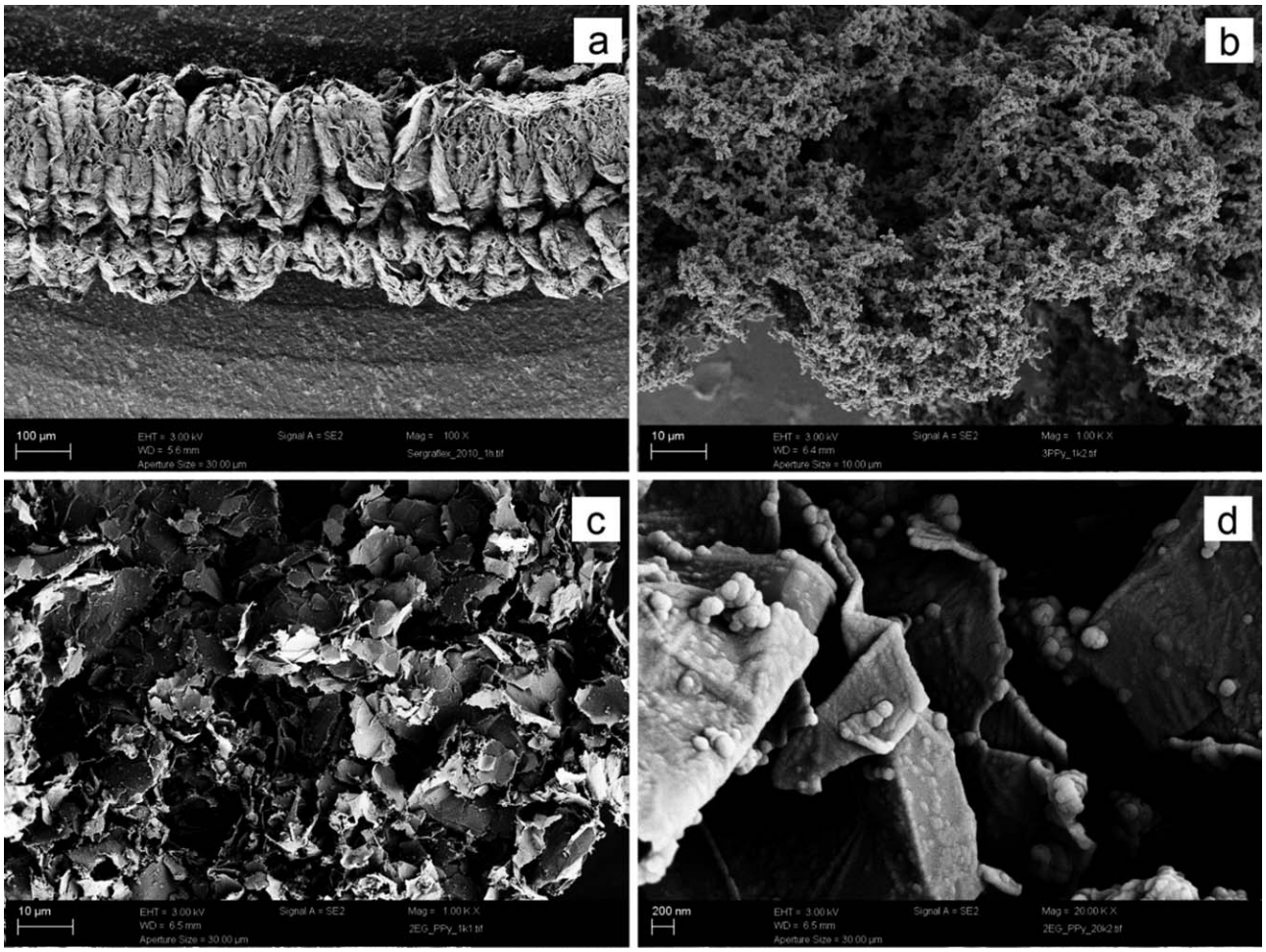

Figure 1. Microstructure of (a) SIGRAFLEX expanded graphite, (b) pure polypyrrole, and (c, d) EG-PPy (1 : 1) composites at different magnifications (SEM).

EXPERIMENTAL

Materials

To analyze the influence of viscosity on network formation and resulting properties, we used in this work two polypropylenes with different viscosities. Table I shows the physical properties of the two polymers.

Expanded graphite SIGRAFLEX Expandat was provided from SGL Technologies GmbH, SGL Group (Germany). Following properties of this filler have been determined: conductivity 40 S/cm (room temperature, 30 MPa, self-made 2-points conductivity tester, coupled with a DMM2000 Electrometer, Keithley Instruments); apparent volume ~400 cm^3/g; specific surface 39.4 m^2/g (77.4 K, N_2 atmosphere, Autosorb-1, Quantachrome). PP and EG were dried at 85°C under vacuum overnight before use. Pyrrole for the synthesis of PPy was supplied by Merck-Schuchardt (Germany) and freshly distilled

Table I. Physical Properties of PPs (Data Provided by the Producers)

PP	HD 214 CF	Novolen 1106H	Norm
Abbreviation	lv-PP	hv-PP	-
Producer	Borealis	Basell	-
Density (g/cm^3)	0.90–0.91	0.9	ISO 1183
MFI (g (10 min) $^{-1}$)	8	2.1	ISO 1133
Young's modulus (MPa)	650–750 [a]	1450[b]	[a]ISO 527-3, [b]–1
Strain at break (%)	500–700 [a]	> 50[b]	[a]ISO 527-3, [b]–1
Stress at break (MPa)	30–50	-	ISO 527-3
Melting point	162–166°C	-	DSC; ISO 3146

Table II. Composition of the Composites, Evaluated from TGA Results

[EG-PPy] (wt %)	$[EG]_{theoretical}$[a] (wt %)	r at 800°C (wt %) Theoretical[b]	Experimental	$[EG]_{experimental}$ (wt %)[c]
lv-PP (HD214 CF)				
2	0.75	1.2	2.5	1.5
4	1.50	2.5	2.5	1.5
6	2.25	3.7	4.8	2.9
8	3.00	4.9	5.5	3.3
12	4.50	7.4	8.6	5.2
16	6.00	9.9	9.7	5.9
20	7.50	12.4	12.1	7.3
hv-PP (PP Novolen 1106H)				
2	0.75	1.2	1.7	1.0
4	1.50	2.5	2.3	1.4
6	2.25	3.7	3.0	1.8
8	3.00	4.9	5.4	3.2
12	4.50	7.4	7.4	4.5
16	6.00	9.9	9.6	5.8
20	7.50	12.4	13.8	8.3

[a] According to eq. (5).
[b] According to eq. (6).
[c] According to eq. (7).

before use. $FeCl_3 \cdot 6\ H_2O$ was supplied by Sigma-Aldrich and 4-dodecyl-benzene sulfonic acid (DBSA) (90%) by Fluka. Both were used without further treatment.

Sample Preparation

Modification of EG with PPy. EG and pyrrole in rapport 1 : 1 (by wt) were mixed to prepare the pre-composite by chemical oxidative *in situ* polymerisation of pyrrole in presence of dispersed EG. 0.438 g DBSA was dissolved in 300 mL distilled water and 0.450 g EG was added to the solution and treated for 2 h by sonication (ultrasonic processor, Hielscher model UP400S, US Finger S7, cycle: 1, amplitude: 55). Then 2.502 g $FeCl_3$ 6 H_2O was added under stirring and 0.450 g of pyrrole was added dropwise into the dispersion. The stirring was kept for 24 h at room temperature. The color of dispersion turned rapidly from grey to black. During the reaction, a slight trend toward agglomeration was visible. The final product was filtered off, washed with about 1 L Millipore water, 100 mL of acetone, and finally dried in vacuum oven at 60°C for 4 h.

Composites Preparation. Fillers were introduced in the polymer matrix by melt mixing using a twin screw DSM 15 cm^3 Micro compounder, DSM Xplore, The Netherlands). For all the samples, the mixing conditions were 200°C, 100 rpm, and 10 min. To prepare samples for the required analyses, the strands obtained from the melt mixing were cut into pellets and compression moulded to plates. The compression moulding conditions were chosen in such a way, that plates without visible voids or heterogeneities were obtained. The polypropylene with the lower viscosity (lv-PP) was compression moulded at 210°C at 50 k*N*, the PP with higher viscosity (hv-PP) at 220°C, 50 k*N*, both for 2 min. Plates of 25 mm diameter and 1.5 mm thickness were prepared for the conductivity and rheological measurements. For the mechanical tests, dog-bone specimens with a stage size of 10 × 2.0 × 1.0 mm^3 were cut from plates of 60 mm diameter and 1.0 mm thickness. For thermal conductivity measurements, cylinders with 13 mm diameter and height of 12 mm were compression moulded by means of a vacuum press PW 20 (Paul-Otto Weber GmbH). The conditions were 210°C and 17.5 k*N* for lv-PP/EG, 210°C and 20 k*N* for lv-PP/EG-PPy, or 200°C and 20 k*N* for hv-PP/EG and hv-PP/EG-PPy, all with slow cooling after pressurization. The samples were cut into 2 pieces of about 6 mm thickness for thermal conductivity tests (TPS method). The cut sides were carefully smoothed mechanically. From the same cylinders, 2 mm thick samples were cut for thermal conductivity tests by laser flash analysis (LFA).

Methods

Scanning Electron Microscopy. The sample structures were analyzed by an SEM Supra 55VPO (Carl Zeiss NTS GmbH). Plates were cooled with liquid N_2 and fractured. The fracture surfaces were smoothed by microtomy using freshly prepared glass knifes. The sample surfaces were sputtered with Pt to hinder electrostatic charging during SEM analysis.

Differential Scanning Calorimetry. The thermograms of the polymers and their composites were obtained by means of a DSC Q1000 calorimeter (TA Instruments) in the temperature range from −80°C to 180°C under nitrogen atmosphere. The mass of the samples was in the range of 4 to 6 mg and the rate used was 10 K/min for both heating and cooling processes. The crystallinities of the composites were normalized to the weight fraction of PP in the composites.

Thermogravimetric Analysis. The exact weight percentage of the EG in the composites where the filler was EG-PPy was determined from the of TGA results obtained by a TGA Q5000 (TA instruments) under nitrogen atmosphere, following a heating method with an isothermal for 5 min at room temperature and then a ramp of 10 K/min up to 800°C. The mass of the samples varied from 3 to 7 mg.

Rheological Measurements. Melt rheological measurements were carried out on plates of 25 mm diameter and 1.5 mm thickness, prepared via compression moulding. An ARES G2 instrument was used using parallel plate geometry. The measurements were done at 200°C under N_2 atmosphere. Oscillation frequency sweeps were performed increasing frequency from 0.1 to 100 rad/s, followed by a sweep decreasing frequency from 100 to 0.03 rad/s. The second sweep was taken for the data analysis.

Mechanical Properties. Tensile tests were performed with a mechanical testing machine Zwick 8195.05 according to DIN EN ISO 527-2 with a strain rate applied of 5 mm/min. The specimens were cut into a dog-bone configuration from plates of 60 mm diameter and 1 mm thickness prepared via compression moulding. The dimensions of the test zone were approximately 1 mm thickness, 2 mm width, and 10 mm length. Given are the mean values of at least 5 tests for each material.

Electrical Conductivity. Volume resistance measurements were carried out on a 6175A Electrometer (Keithley Instruments), coupled with an 8009 Resistivity Test Fixture with two plate

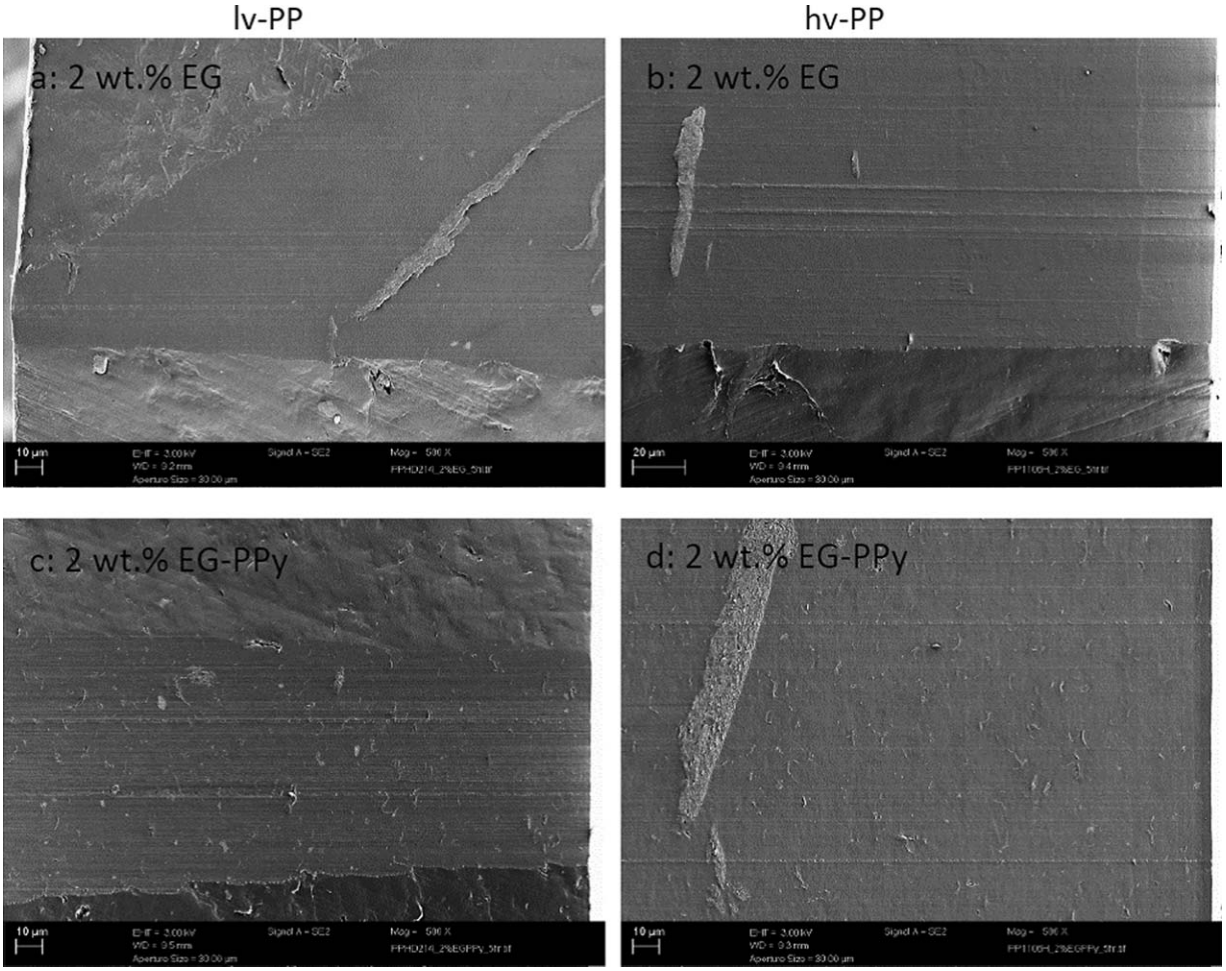

Figure 2. Morphology of PP/EG and PP/EG-PPy composites containing 2 wt % filler (SEM, surfaces of cryofractures of plates smoothed by microtomy; left lv-PP, right hv-PP composites; filler type is given in the figures).

electrodes located on both sides of the samples. The resistance R_v was converted to volume resistivity ρ_v using the formula:

$$\rho_v = \frac{\pi d^2}{4l} R_v \tag{3}$$

where d is the diameter, l the thickness and R_v is the measured resistance. The conductivity σ_v (or simply σ) we subsequently calculated as the inverse of the resistivity ρ_v (2E-method). According to ASTM D257-07 this method is suitable for resistance values in the range 10^7-10^{18} Ω corresponding to conductivity values of about 10^{-19} to 10^{-8} S/cm, but reliable results can be obtained up to 10^{-4} S/cm.

Thermal Conductivity. Measurements of the thermal conductivity κ were performed with a Hot Disk TPS 500 Instrument (Thermal Test Inc.). The used sensor had a radius of 3.189 cm and the dimensions of the samples prepared were 13 mm diameter and 5–6 mm thickness. The sensor was placed between two samples faced to cut side or faced the moulded side of the samples (see sample preparation). We could not detect significant differences of the thermal conductivity parameters between the two arrangements. The parameters used for the calculation of κ were obtained with a probing depth < 3.5 mm and a temperature increase between 5 and 10°C. The power and duration of the impulse were varied to fit these conditions (setting parameters: 100 or 200 mW; 2.5–20 s). Each sample was measured at least 4 times.

Since the heat capacity of the sensor itself may falsify the results, especially at low conductivity values, we repeated thermal conductivity measurements with a LFA 447 Instrument (NETSCH Group) equipped with a Xenon NanoFlash laser and an InSb IR sensor (specimen holder 12,7rd). Specimen dimensions of about 2 mm thickness and 13 mm diameter were cut from the same samples analyzed before by the TPS 500. All samples were coated with gold because pure PP are transparent to the laser. To obtain a complete and homogeneous absorption of the laser energy, the specimens were sprayed with graphite (Graphit33 Leitpack, Kontakt Chemie, CRC Industries Inc.).

RESULTS AND DISCUSSION

Determination of EG Concentration in PP/EG-PPy Composites by TGA

The measurement of the real concentration of expanded graphite, [*EG*], in the EG-PPy based composites has been done by TGA evaluating the residues at 800°C (in wt %) (Table II).

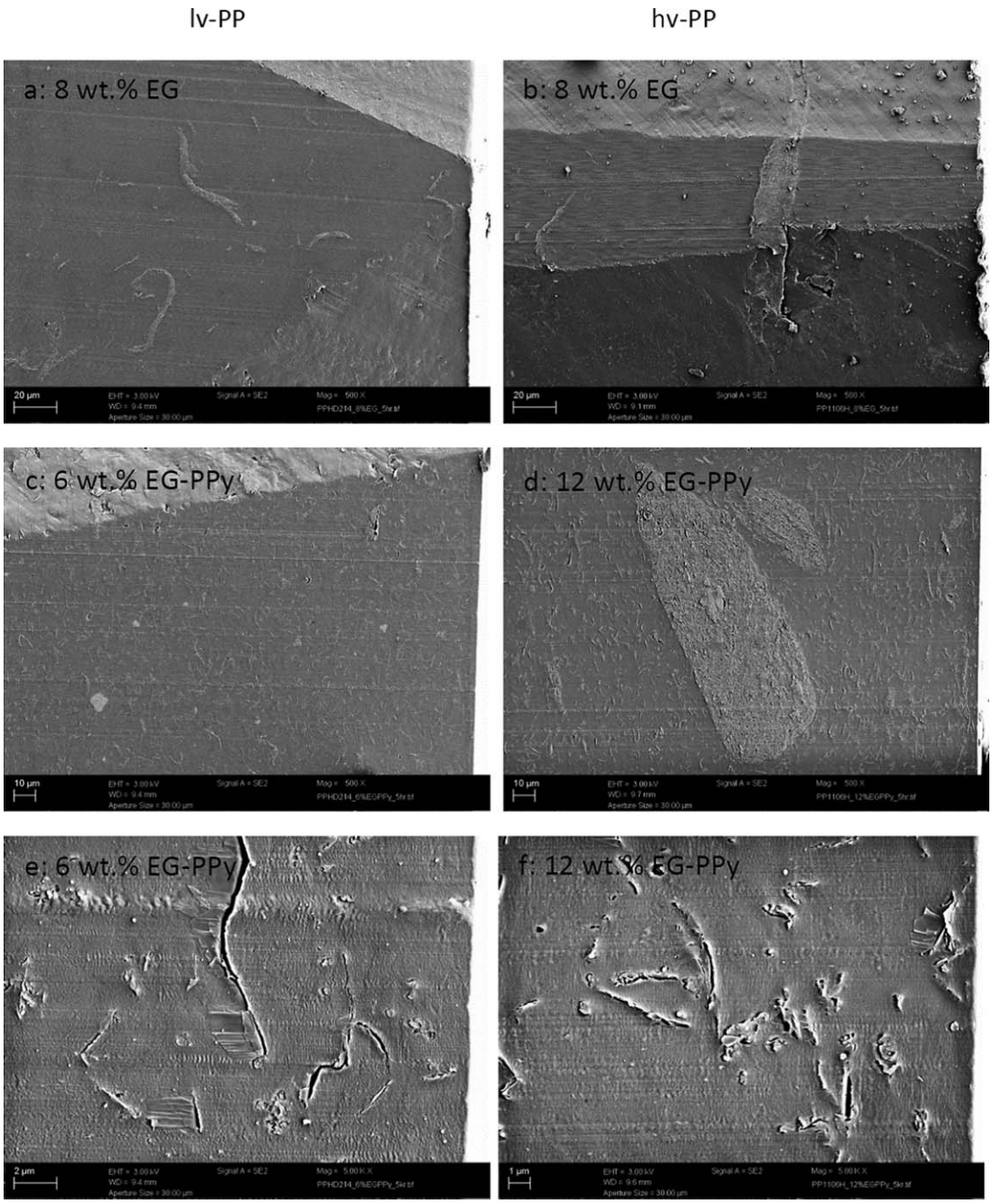

Figure 3. Morphology of PP/EG and PP/EG-PPy composites near to the electrical percolation concentration (SEM, surfaces of cryofractures of plates smoothed by microtomy; left lv-PP, right hv-PP composites; filler concentration and type are given in the figures).

Since the graphite does not show any phenomena in the temperature range of TGA, its residue r_{EG} can be approximated to be 100 wt %. The pure PPy sample shows a residue r_{PPy} of 38.9 wt %, while the composite EG-PPy(1 : 1) has a residue $r_{EG\text{-}PPy}$ of 61.8 ± 1.4 wt %. Assuming additive behavior of the decomposition process, the EG content in the EG-PPy(1 : 1) composite can be calculated as

$$[EG]_{EG\text{-}PPy} = \left(\frac{r_{EG\text{-}PPy} - r_{PPy}}{r_{EG} - r_{PPy}}\right) \text{wt \%} = \left(\frac{61.8 - 38.9}{100 - 38.9}\right) \text{wt \%} = 37.5 \text{ wt \%} \quad (4)$$

This calculation does not consider that EG may modify the degradation of PPy and of the other reagents, $FeCl_3$ and DBSA, inevitably present in the sample. Since PP decomposes completely under the used TGA conditions, the theoretical EG contents in the PP/EG-PPy composites we estimated by eq. (5) and the theoretical residue after TGA is according to eq. (6) ([EG-PPy] is the concentration of the EG-PPy added to the composite):

$$[EG]_{theoretical} = \frac{[EG-PPy]}{100}[EG]_{EG\text{-}PPy} \text{ wt \%} = \frac{[EG-PPy]}{100} 37.5 \text{ wt \%} \quad (5)$$

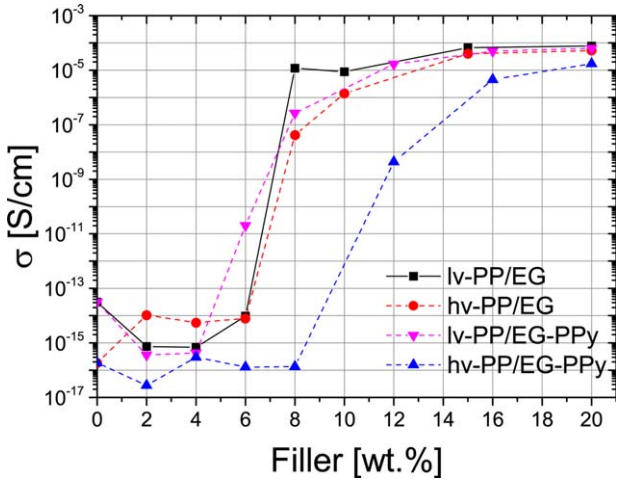

Figure 4. Electrical conductivity of PP/EG and PP/EG-PPy composites as function of the filler concentration. [Color figure can be viewed in the online issue, which is available at wileyonlinelibrary.com.]

$$r_{\text{theoretical}} = \frac{[\text{EG}-\text{PPy}]}{100\ \%}\, r_{\text{EG-PPy}}\,\text{wt}\ \% = \frac{[\text{EG}-\text{PPy}]}{100\ \%}\ 61.5\ \text{wt}\ \% \quad (6)$$

Eventually, from the experimental residues we calculated EG contents according to eq. (7).

$$[EG]_{\text{experimental}} = \frac{r_{\text{experimental}}}{r_{\text{EG-PPy}}}\,[\text{EG}]_{\text{EG-PPy}}\,\text{wt}\ \% = \frac{r_{\text{experimental}}}{61.8}\ 37.5\ \text{wt}\ \% \quad (7)$$

In all these calculations, eventual mutual interference among the components during the thermal degradation is not considered. However, there is a rather good agreement between the values expected from the feed composition and those evaluated experimentally by TGA (Table II). The experimental and calculated EG contents differ with an average standard deviation of < 0.3, which is a good result despite the approximations and experimental uncertainties.

Morphology. The structure of EG-PPy composite was investigated and was compared with the structure of the pure EG and PPy to verify the resulting morphology and stability of the coating. Figure 1(a) shows the worm-like structure of EG used for the modification with PPy and for the preparation of the PP-EG composites. The structure is built from graphite nanoplatelets (GNP) stacking loosely together, and is very porous. The diameter of the "worms" is a few 100 μm and their length is in a broad range up to mm. Under shear or due to sonication the worms decompose to free GNP (10 nm to few 10 nm in thickness and few 10 μm in lateral dimension), which are anisotropically packed after filtration (similar as in Figure 1(c), the PPy coated GNP). The PPy also shows a very porous and well-defined structure [Figure 1(b)] grown as a dendritic arrangement of spherulites, when the PPy is prepared in solution. When pyrrole is polymerized in presence of the dispersed GNP, such open PPy structures are not visible anymore. Figure 1(c) shows the loose and disordered arrangement of the GNP, which are coated by spherulitic structures (diameter 100–200 nm) grown from the GNP surface, as can be seen at higher magnification [Figure 1(d)]. PPy is covering the GNP completely; no plain GNP surface is visible after this coating process anymore.

When incorporating the filler into the PP matrices by melt mixing, we observed very different morphologies, depending on the filler type and melt viscosity. Pure EG forms larger anisotropic agglomerates, a few μm thick and up to 100 μm long in the plane. Smaller particles in the size of GNP are hardly detectable [Figure 2(a,b)]. The situation was different when adding EG-PPy; beside few big agglomerates in case of the hv-PP mainly small particles in the size of GNP are homogeneously dispersed in the PP matrices [Figure 2(c,d)]. Obviously the PPy coating is helpful in the dispersion process of the EG.

When increasing the filler concentration above the electrical percolation concentration (see below: "Electrical and thermal conductivity"), the morphology of the conductive paths is also very different (Figure 3). Without PPy, big agglomerates, up to 20 μm thick and up to a few 100 μm long, form the paths, especially in hv-PP. In lv-PP, the anisotropic EG agglomerates are much smaller and more homogeneous distributed in the

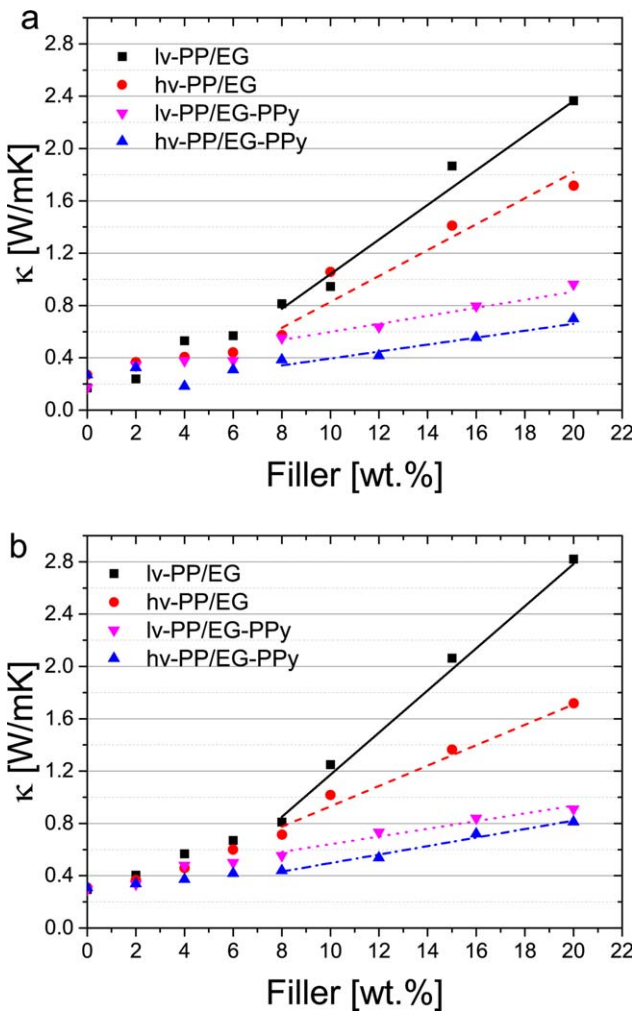

Figure 5. Thermal conductivity of PP/EG and PP/EG-PPy composites as function of the filler concentration: (a) LFA 447 Analysis; (b) Hot Disk TPS 500. [Color figure can be viewed in the online issue, which is available at wileyonlinelibrary.com.]

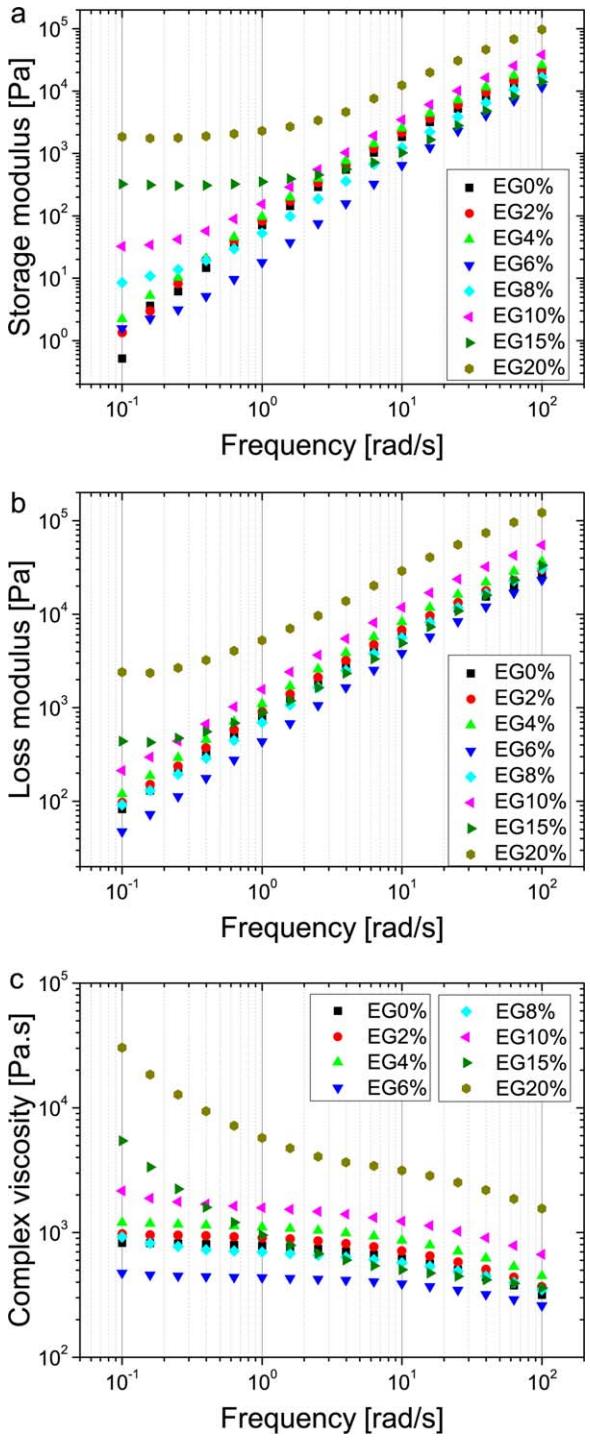

Figure 6. Viscosity dependence of lv-PP/EG-PPy composites on filler concentration and frequency; (a) storage modulus, (b) loss modulus, and (c) complex viscosity. [Color figure can be viewed in the online issue, which is available at wileyonlinelibrary.com.]

matrix and also isolated GNP can be detected. After melt mixing EG-PPy with PP almost only GNP structures are detected in case of lv-PP, while in hv-PP a mixture of big agglomerates and isolated and homogeneous dispersed GNP is formed. In higher magnification [Figure 3(e and f)] one can see that the dispersed GNP consist mainly of pure graphene layers with some 10 nm-dimension in thickness and some μm dimension in the plane. Due to the weak graphene interlayer forces, during the surface cut preparation some graphene is pulled out from the GNP and is laying now as flat structure on the sample surface. The weak interlayer forces are also the reason for the decomposition of the EG-PPy structure during the melt mixing process. The PPy coating is just sheared off, however, the PPy location and distribution in the composite could not be analyzed with the used techniques.

Electrical and Thermal Conductivity. Below the percolation concentration PC, the conductivity σ is less than 10^{-13} S/cm, at PC it increases by about 7–8 orders of magnitude up to 10^{-6} S/cm (Figure 4). The difference in viscosity does not influence the percolation concentration of the two series of samples with EG, which is between 6 and 8 wt % EG. This range is in rather good agreement with the electrical percolation observed by Li *et al.* for PP/EG composites prepared by precipitation from solution.[32] In contrast, the viscosity of the matrix plays an important role for the formation of conducting paths in EG-PPy containing composites. The percolation threshold is lower in lv-PP/EG-PPy composites than in hv-PP/EG-PPy. We could not observe big agglomerates at the PC of lv-PP/EG-Py [Figure 3(c)], while hv-PP/EG-Py still contains big agglomerates [Figure 3(d)] at PC, certainly the reason for the higher PC value. That means that the better wetting behavior due to lower viscosity is favorable for the dispersion of the filler and that the weaker forces acting on the particles during melt mixing are strong enough to degrade the agglomerates resulting in a fine dispersion of the filler without destroying the percolation paths.

The PP/EG-PPy composites are already conductive with 4.5 wt % EG (corresponding to 12 wt % EG-PPy, compare to Table II) in case of hv-PP and 3 wt % EG (corresponding to 8 wt % EG-PPy) in case of lv-PP. This demonstrates that the intrinsic conductive PPy contributes fundamentally to the formation of the percolation paths and that there is a synergistic effect between EG and PPy with regard to electrical conductivity. Please note that for melt mixed composites of PP with PPy, prepared by chemical oxidative polymerization, very high loadings are necessary to reach electrical conductivity and even at a weight content of 35% PPy σ does not exceed 1×10^{-7} S/cm.[33]

The measurements of thermal conductivity κ show a completely different behavior compared to electrical conductivity. Laser flash analysis of the thermal conductivities dependence on filler content gives for all composites a linear increase of κ up to 8 wt % loading [Figure 5(a)]. The increase is stronger in the case of EG filler compared to the EG-PPy filler. In lv-PP the increase is about 200%, in hv-PP about 120% and in the corresponding EG-PPy containing composites roughly only half of these values. Above 8 wt % the slopes of the κ-EG-dependence are almost the same for the composites containing EG-PPy, but the curves shift to higher slopes when only EG is present in the composites. At these concentrations, the thermal percolation concentration, paths for phonon transport through the sample are formed without phase boundaries between the strongly conductive EG and weakly conductive matrix. With 20 wt % EG the thermal conductivity is nearly 9 times of that of neat lv-PP and

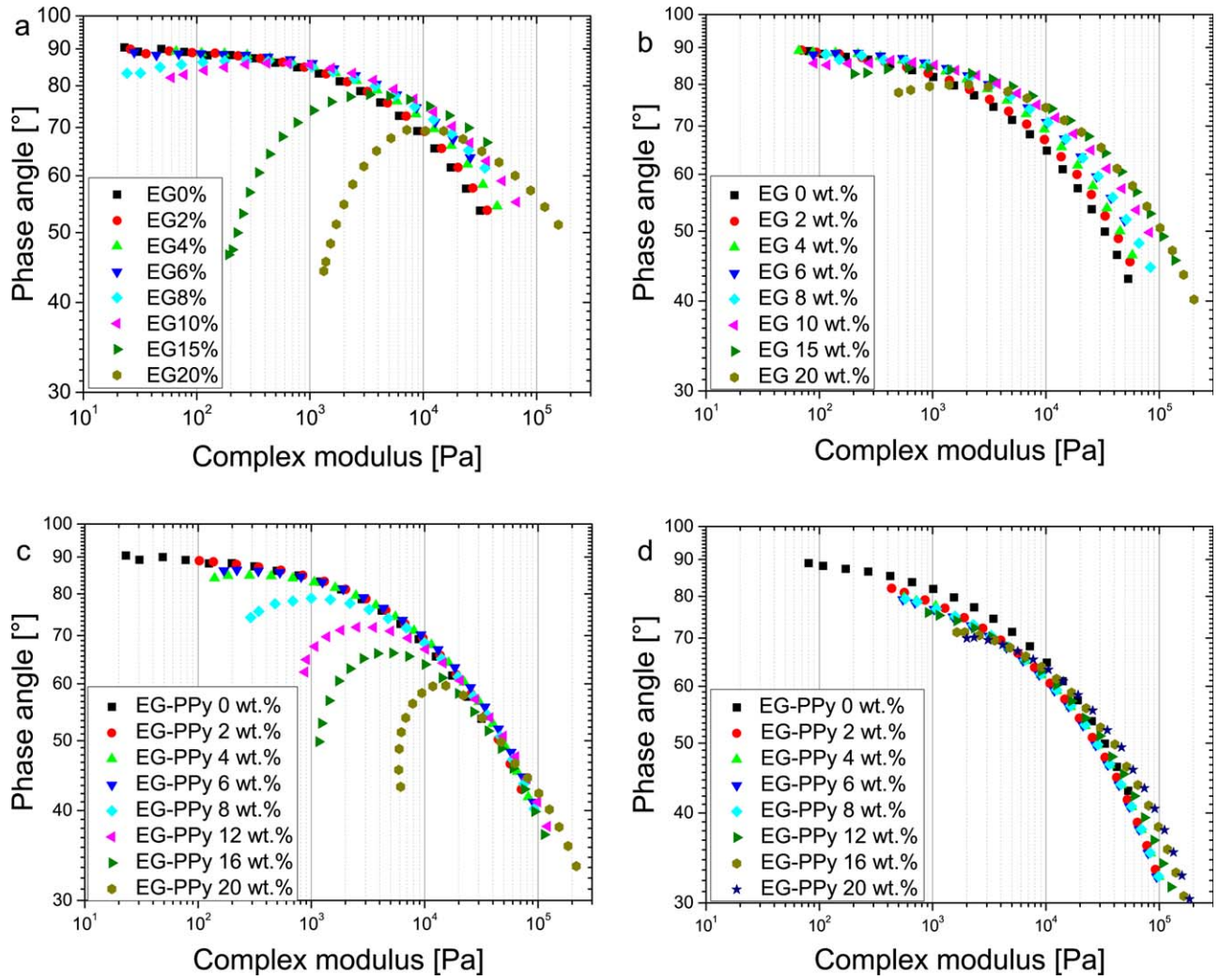

Figure 7. Van Gurp-Palmen plots of (a) lv-PP/EG composites, (b) hv-PP/EG composites, (c) lv-PP/EG-PPy composites, and (d) hv-PP/EG-PPy composites. [Color figure can be viewed in the online issue, which is available at wileyonlinelibrary.com.]

7 times of that of neat hv-PP. The thermal conductivity of the PP/EG composites with more than 10 wt % EG are above 1 Wm/K and thus this material becomes suitable for heat management applications.[34] At 20 wt % (less than 10 vol %) EG the thermal conductivity is about 2.5 Wm/K and in the same range observed by Fukushima *et al.* for polyamide 6 containing 15 vol % EG.[34] 20 wt % EG-PPy increases κ only by 3.2 or 2.7 times in lv-PP or hv-PP, respectively. This low thermal conductivity was surprising but it opens the possibility for development of thermoelectric material based on polymer composites, which requires good electrical but poor thermal conductivity.[35]

To be sure that this observation is not an artefact we repeated the heat conductivity measurements with the *Hot Disk TPS 500* [Figure 5(b)]. We are aware that the results obtained with the used geometry of the samples may be affected by the heat capacity of the sensor, but the tendency should be the same. Indeed, the shape of the curves is very similar with a tendency to higher conductivity values determined with this method. A slight shift in the slope of the curve seems to be present also in the hv-PP/EG-Py sample but most important, no influence of the contact side of the samples to the sensor, either the mould side or the cut side, was found, demonstrating the homogeneity of the composite morphology.

Comparing the measured thermal conductivity values of the PP/EG-PPy composites with the EG content of the composites (Table II) it becomes obvious that only EG contributes to the thermal conductivity, the effect of PPy is only marginal, if any. PP/EG-PPy composites have very similar thermal conductivities as the PP/EG composites containing the same EG content. The slight tendency to higher values is possibly due to the better dispersion of EG in PP/EG-PPy composites.

Rheology. The rheological analysis showed an increase in both storage modulus G′ and loss modulus G″ as function of the filler concentration especially at low frequencies f, which confirms the general behavior of graphite[36] or EG composites.[32,37] There are no marked differences between EG and EG-PPy fillers. Exemplary, plots describing the rheological behavior of lv-PP/EG composites are shown in Figure 6. The percolation, that means the formation of a network-like arrangement of the filler

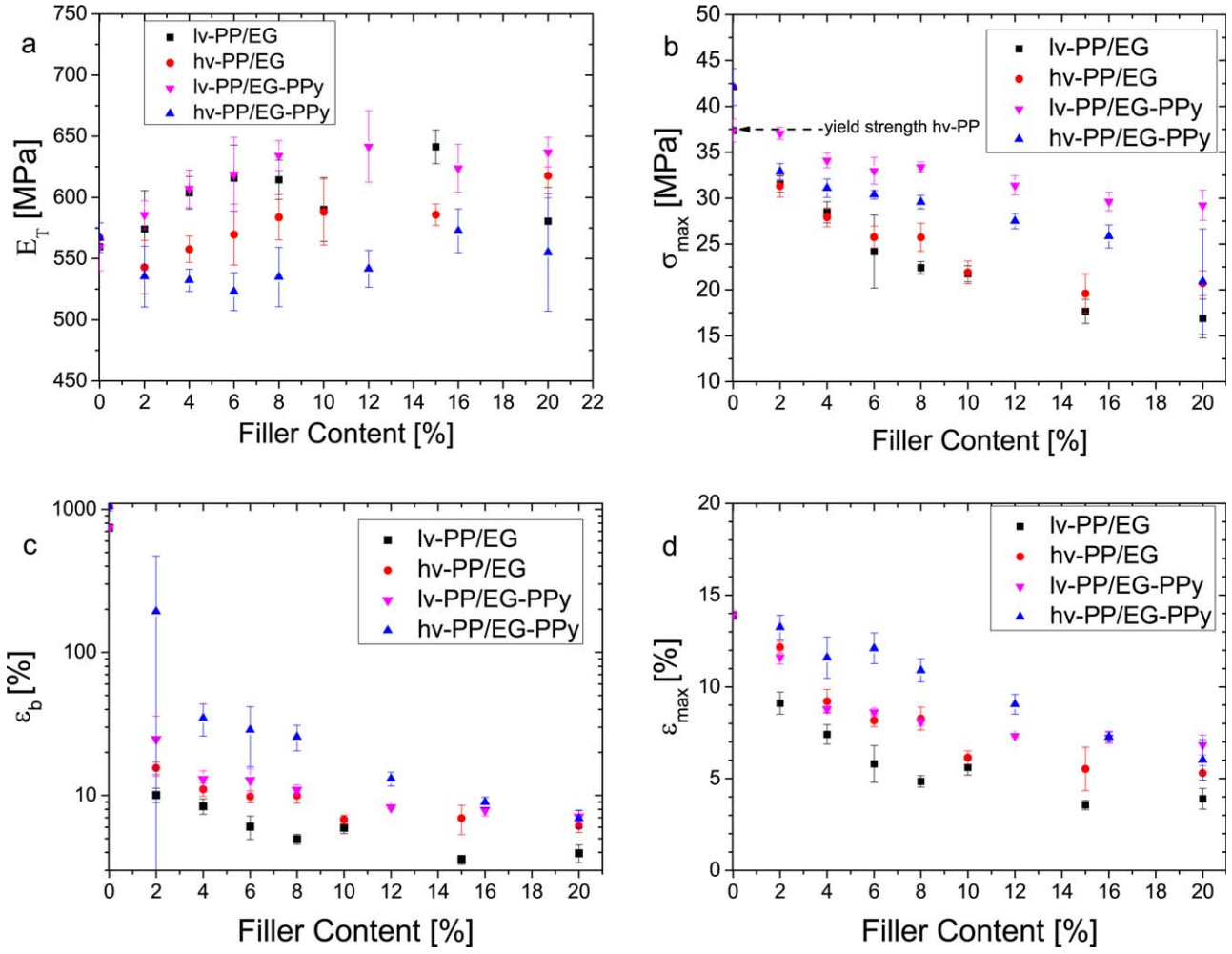

Figure 8. Mechanical properties of PP/EG and PP/EG-PPy composites in dependence on filler content. (a) Young's modulus; (b) yield strength; (c) elongation at break; (d) elongation at yield. [Color figure can be viewed in the online issue, which is available at wileyonlinelibrary.com.]

in the polymer melt, is detected in the low frequency range as plateau formation in the G'-f- and G''-f plots or as positive deviation of the complex viscosity γ from the plateau level in the γ-f plot. From these plots one can conclude on the formation of percolating network structures at 6 wt % (G'-f plot), 10 wt % (γ-f plot), or 15 wt % filler (G''-f plot). More sensitive to "rheological percolation" is the plot of the phase angle versus the complex modulus, the "Van Gurp-Palmen plot,"[38,39] shown in Figure 7. As long as no filler network is present, the phase angle reduces continuously with increasing complex modulus. When a filler network is present, a maximum in the curve is observed. Clearly, strong differences in rheological percolation can be seen. The lower viscosity polypropylene filled with EG has lower percolation (< 8 wt %) than the higher viscosity one (ca. 10 wt %). These values are somehow lower than the rheological percolation observed in PP/EG composites prepared from solution but in the same order.[32] When substituting EG with EG-PPy in the case of hv-PP the percolation is shifted to higher filler content (ca. 15 wt %), which can be expected since the filler is a mixture of anisotropic GNP and more or less isotropic PPy. In contrast, for lv-PP a shift to even lower percolation is observed (< 4 wt %). In this case the percolating network must be based on EG and PPy. The same we assume for the hv-PP/EG-PPy composites, but in these composite the big agglomerates (see Figure 3) reduce the particle number density in the matrix and larger amounts of filler are necessary for network formation.

Mechanical Properties. The morphology of the composites, i.e. the dispersion and distribution of the filler and the crystallinity of the polymer matrix, influence the mechanical properties of the composites. Tensile tests have been performed to determine Young's modulus E_t, yield strength and elongation at yield, and stress and strain at break. The applied processing conditions resulted in very ductile pure PPs with elongation at breaks of 740% and 1050% for lv-PP and hv-PP, respectively. Both polymers show yielding, necking and strain hardening. lv-PP has a yield stress of 37.4 (±1.3) MPa (at $\varepsilon = 13.9$ (±0.3) %) and the stress at break is 34.9 (±1.5) MPa, these of hv-PP are 35.1 (±0.3) MPa (at $\varepsilon_y = 15.2$ (±0.1) %) and 42.0 (±2.0) MPa, respectively.

When fillers are added, the stress–strain behavior is strongly changed. First, there is a tendency to increased E_t values with increasing filler content [except for hv-PP/EG-PPy composites,

Figure 8(a)] but the increase is much less than what was observed with other bi-dimensional fillers, e.g. clays.[40] The increase is significant for lv-PP composites and PPy contributes to it more strongly than the added EG. The yield strength (which is 35.1 MPa for hv-PP) decreases continuously with added filler concentration, especially in case of added pure EG [Figure 8(b)]. This is certainly due to the agglomerated structures in the PP/EG composites which are much bigger than in the PP/EG-PPy composites (Figures 2 and 3). The formation of agglomerates is also the reason for the fracture at low elongations, which is shifted more to the yield point with increasing filler contents [Figure 8(c)]. The layered structure of the expanded graphite and its graphite nanosheets allows the formation of nanoporosity (or nanovoids) among the platelets,[41] which are able to act like focal sites of failure when the material is tested under stress conditions.[42] Since in the PP/EG-PPy composites the agglomerates are much smaller, the reduction in the elongation at break is less drastic. Overall, the composites still show rather ductile behavior with yield elongations of some % even at high filler contents [Figure 8(d)]. In summary, the addition of the conductive fillers has negative effects on the mechanical strength. Pure EG is more detrimental on the mechanical properties than the mixture of EG and PPy.

CONCLUSIONS

The addition of expanded graphite (EG) is a suitable way to introduce electrical and thermal conductivity to intrinsically electrically and heat insulating polypropylenes. However, this addition is detrimental to mechanical strength of the formed composites. Modification of the EG with polypyrrole (PPy) resulted in a complete coating of the graphite nanoplatelets (GNP). The addition of this EG-PPy filler is less harmful to the mechanical strength of PP than the addition of pure EG. Even if the EG-PPy structure is not stable during melt mixing, the presence of PPy helps in the fine dispersion of the EG and hinders the formation of big agglomerates.

In the PP/EG-PPy composites PPy contributes to the formation of electrical conductive paths but not to heat transfer. This combination of high electrical conductivity and poor thermal conductivity is advantageous for applications as thermoelectric material, which will be studied more in detail in future. PPy and EG exhibit a synergistic effect with regard to electrical percolation and conductivity, but this effect is strongly dependent on the matrix viscosity and very strong in case of low viscous PP (lv-PP). The synergistic effect of EG and PPy also becomes clear when analyzing the melt viscosity, which shows a strong contribution of the PPy to the filler network formation especially in case of the low viscous PP. Overall, there is a good correlation between electrical, thermal and rheological percolation observed in the PP/EG and PP/EG-PPy composites.

ACKNOWLEDGMENTS

This work was financially supported by the Deutsche Forschungsgemeinschaft (DFG; Project PI 308/9-1), by the National Research Foundation of South Africa and the International Bureau of the BMBF in Germany (project SUA 10/009), and by the Deutscher Akademischer Austauschdienst (DAAD, PPP Slowakei 2j ab 13). The SGL Carbon is appreciated for providing the expanded graphite. The authors thank their colleagues from Leibniz IPF Dresden for their help, Liane Häußler for thermal characterisation, Holger Scheibner for mechanical tests, and Helfried Kunath for recording SEM and optical images as well as for his general technical assistance.

REFERENCES

1. Stauffer, D. Introduction to Percolation Theory; Taylor and Francis: London, **1985**.
2. Youngs, I. J. *J. Phys. D: Appl. Phys.* **2002**, *35*, 3127.
3. Salazar, A.; Sanchez-Lavega, A.; Terron, M. J. *J. Appl. Phys.* **1998**, *84*, 3031.
4. Kole, M.; Tripathi, D.; Dey, T. K. *Bull. Mater. Sci.* **2012**, *35*, 601.
5. Ganguli, S.; Roy, A. K.; Anderson, D. P. *Carbon* **2008**, *46*, 806.
6. Kasgoz, A.; Dincer, A.; Durmus, A. *Polym. Eng. Sci.* **2012**, *52*, 2645.
7. Gurp, M. V.; Palmen, J. *Rheol. Bull.* **1998**, *67*, 5.
8. Pötschke, P.; Abdel-Goad, M.; Alig, I.; Dudkin, S.; Lellinger, D. *Polymer* **2004**, *45*, 8863.
9. Heo, S. I.; Yun, J. C.; Oh, K. S.; Han, K. S. *Adv. Compos. Mater.* **2006**,*15*, 115.
10. Nanni, F.; Ruscito, G.; Puglia, D.; Terenzi, A.; Kenny, J.,M.; Gusmano, G. *Comp. Sci. Technol.* **2011**, *71*, 1.
11. Kasaliwal, G.; Göldel, A.; Pötschke, P. *J. Appl. Polym. Sci.* **2009**, *112*, 3494.
12. Yakovlev, A. V.; Finaenov, A. I.; Zabud'kov, S. L.; Yakovleva, E. V. *Russ. J. Appl. Chem.* **2006**, *79*, 1741.
13. Zheng, W.; Lu, X. H.; Wong, S. C. *J. Appl. Polym. Sci.* **2004**, *91*, 2781.
14. Li, Y.; Zhu, J.; Wei, S.; Ryu, J.; Wang, Q.; Sun, L.; Guo, Z. *Macromol. Chem. Phys.* **2011**, *212*, 2429.
15. Tryba, B.; Kalenczuk, R. J.; Kang, F. Y.; Inagaki, M.; Morawski, A. W. *Mol. Cryst. Liq. Cryst.* **2000**, *340*, 113.
16. Zhan, D.; Ni, Z. H.; Chen, W.; Sun, L.; Luo, Z. Q.; Lai, L. F.; Yu, T.; Wee, A. T. S.; Shen, Z. X. *Carbon* **2011**, *49*, 1362.
17. Chen, G. H.; Weng, W. G.; Wu, D. J.; Wu, C. L.; Lu, J. R.; Wang, P. P.; Chen, X. F. *Carbon* **2004**, *42*, 753.
18. Kalaitzidou, K.; Fukushima, H.; Drzal, L. T. *Carbon* **2007**, *45*, 1446.
19. Kalaitzidou, K.; Fukushima, H.; Askeland, P.; Drzal, L. T. *J. Mater. Sci.* **2008**, *43*, 2895.
20. Kalaitzidou, K.; Fukushima, H.; Drzal, L. T. *Compos A Appl. Sci. Manuf.* **2007**, *38*, 1675.
21. Abdel-Goad, M.; Potschke, P.; Zhou, D. H.; Mark, J. E.; Heinrich, G. *J. Macromol. Sci. Part A: Pure Appl. Chem.* **2007**, *44*, 591.
22. Srivastava, N. K.; Sachdev, V. K.; Mehra, R. M. *J. Appl. Polym. Sci.* **2007**, *104*, 2027.
23. Omastova, M.; Trchova, M.; Kovarova, J.; Stejskal, J. *Synth. Met.* **2003**, *138*, 447.

24. Omastova, M.; Pionteck, J.; Kosina, S. In Electronic and Optical Properties of Conjugated Molecular Systems in Condensed Phases; Hotta, S., Ed.; Research Signpost: Trivandrum, **2003**; Chapter 6, pp 153–186.
25. Omastova, M.; Micusík, M.; Fedorko, P.; Chehimi, M. M.; Pionteck, J. *Mater. Sci. Forum* **2010**, 636, 676.
26. Omastova, M.; Micusik, M. *Chem. Papers* **2012**, *66*, 392.
27. Yanai, N.; Uemura, T.; Ohba, M.; Kadowaki, Y.; Maesato, M.; Takenaka, M.; Nishitsuji, S.; Hasegawa, H.; Kitagawa, S. *Angew. Chem. –Int. Ed.* **2008**, *47*, 9883.
28. Liu, X. H.; Wu, H. Y.; Ren, F. L.; Qiu, G. Z.; Tang, M. T. *Mater. Chem. Phys.* **2008**, *109*, 5.
29. Diez, I.; Emmerling, F.; Malz, F.; Jager, C.; Schulz, B.; Orgzall, I. *Mater. Chem. Phys.* **2008**, *112*, 154.
30. Mravcakova, M.; Boukerma, K.; Omastova, M.; Chehimi, M. M. *Mater. Sci. Eng. C-Biomimetic Supramol. Syst.* **2006**, *26*, 306.
31. Pandis, C.; Logakis, E.; Peoglos, V.; Pissis, P.; Omastova, M.; Mravcakova, M.; Janke, A.; Pionteck, J.; Peneva, Y.; Minkova, L. *J. Polym. Sci. Part B: Polym. Phys.* **2009**, *47*, 407.
32. Li, Y.; Zhu, J.; Wei, S.; Ryu, J.; Sun, L.; Guo, Z. *Macromol. Chem. Phys.* **2011**, *212*, 1951.
33. Omastova, M.; Chodak, I.; Pionteck, J. *Synth. Met.* **1999**, *102*, 1251.
34. Fukushima, H.; Drzal, L.; Rook, B.; Rich, M. *J. Thermal Anal. Calorimetry* **2006**, *85*, 235.
35. He, M.; Qiu, F.; Lin, Z. *Energy Environ. Sci.* **2013**, *6*, 1352.
36. Kasgoz, A.; Akin, D.; Durmus, A. *Polym. Eng. Sci.* **2012**, *52*, 2645.
37. Kim, H.; Macosko, C. W. *Macromolecules* **2008**, *41*, 3317.
38. Trinkle, S.; Friedrich, C. *Rheol. Acta* **2001**, *40*, 322.
39. Trinkle, S.; Walter, P.; Friedrich, C. *Rheol. Acta* **2002**, *41*, 103.
40. Tarapow, J. A.; Bernal, C. R.; Alvarez, V. A. *J. Appl. Polym. Sci.* **2009**, *111*, 768.
41. Sengupta, R.; Bhattacharya, M.; Bandyopadhyay, S.; Bhowmick, A. K.; *Prog. Polym. Sci.* **2011**, *36*, 638.
42. Yasmin, A.; Luo, J. J.; Daniel, I. M. *Comp. Sci. Technol.* **2006**, *66*, 1182.